CHEMISTRY OF MATERIALS

COMMUNICATION

pubs.acs.org/cm

Synthesis and Thermoelectric Properties of Thin Film Assemblies of Bismuth Telluride Nanopolyhedra

Arup Purkayastha,[‡] Abhishek Jain,[†] Claudiu Hapenciuc,[†] Rok Buckley,[†] Binay Singh,[‡] C. Karthik,[‡] Rutvik J. Mehta,[‡] Theodorian Borca-Tasciuc,[†] and Ganpati Ramanath[‡,*]

[‡]Department of Materials Science and Engineering and [†]Department of Mechanical Aerospace and Nuclear Engineering, Rensselaer Polytechnic Institute, Troy, New York 12180, United States

Supporting Information

KEYWORDS: bismuth telluride, thermoelectrics, nanocrystals, assembly, solvothermal, thin film

Thermoelectric materials are of interest[1] for potential use as heat dissipating conduits for cooling hot-spots in nanodevices and generating electrical power from waste heat, for example, released in automobile and aircraft engines and power stations. Bismuth telluride-based alloys exhibit the highest room-temperature figure of merit ZT ~ 1, given by $\sigma\alpha^2 T/\kappa$, where σ is the electrical conductivity, α the Seebeck coefficient, T the absolute temperature, and κ the thermal conductivity.[2] Nanostructuring is a promising strategy to increase ZT due to κ reduction arising from increased phonon scattering at surfaces and interfaces and increase in $\alpha^2\sigma$ due to quantum effects.[2,3] This approach has been demonstrated in thin film and self-assembled quantum dot superlattices[4,5] via nanostructuring in one- or two-dimensions.[6]

Nanoparticle assemblies allow three-dimensional confinement that can lead to even higher ZT values through further reductions in κ, as shown for bismuth antimony telluride alloy pellets obtained from nanoparticles.[7] Tailoring particle size, shape, and crystallinity is key to controlling the thermal and electrical transport properties of such assemblies. Faceted nanocrystals provide opportunities to increase ZT by decreasing the lattice thermal conductivity[8] κ_L and access anisotropic quantum effects.[9,10] For example, nanoparticles with octahedral and tetrahedral shapes can yield lower κ_L than spherical nanoparticles[8] besides opening up possibilities to enhance packing efficiency.

Here, we describe the scalable solvothermal synthesis and assembly of faceted bismuth telluride nanocrystal tetrahedra and octahedra of controllable sizes and study the thermoelectric transport properties of their thin film assemblies. Our results show low κ in thin film nanoparticle assemblies but also low $\alpha^2\sigma$. Further refinement of shape selection and devising treatments to increase packing efficiencies would pave a way for enhancing the thermoelectric properties of thin film assemblies.

We synthesized polyhedral faceted bismuth telluride nanocrystals by decomposing salts of bismuth acetate and trioctylphosphine (TOP)-ligated tellurium. In a typical synthesis, refluxing bismuth acetate in dodecane mixed with oleylamine and oleic acid results in a pale yellow solution due to bismuth−oleylamine complexing.[11] A clear Te-TOP solution was rapidly injected to the bismuth solution under constant stirring. Bismuth−amine complex decomposition and reaction with Te-TOP yields oleic acid-capped Bi_2Te_3 nanocrystals. Physisorbed oleylamine and excess oleic acid were removed by repeated washing and centrifuging in a hexane−isopropanol mixture.

The nanoparticles are faceted polyhedra (see Figure 1a−d) whose size increases with reaction time (see Supporting Information Figure S1). About 30% of the nanoparticles show tetrahedral facets (Figure 1c), while 70% exhibit octahedral facets (Figure 1d). The electron diffraction spot patterns from electron transparent nanoparticle apexes (Figure 2a) indicate that each nanoparticle is a single crystal with fourfold symmetry along the $[5\bar{5}1]$ direction, as confirmed by high-resolution TEM (Figure 2b). This result is consistent with the octahedral shape and coordination seen in the $[5\bar{5}1]$ projection of the rhombohedral unit cell[12] of Bi_2Te_3 (Figure 2c) verified by X-ray diffractograms (Figure 2d). Figure 2e shows the growth habit of the octahedra with reference to the Bi_2Te_3 structure.

The observation of a thin surface casing on the nanostructures in TEM images (Supporting Information Figure S2) suggests surfactant passivation of the nanocrystal surfaces. Core-level spectra from the nanocrystal assemblies obtained by XPS showing C 1s sub-band signatures of carboxyl and methylene moieties of oleic acid at 285.6 and 284.8 eV, respectively, confirm that oleic acid caps the nanocrystal surfaces (Figure 3a). The carboxyl signature is undetectable in samples synthesized without oleic acid. Since the N 1s band is below the detection limit, we infer that oleylamine mainly serves as a complexing agent during synthesis. The presence of Bi 4f (Figure 3b) peaks at 157.4 and 162.6 eV from unoxidized bismuth telluride, and the higher energy bands at 158.9 and 164.1 eV from its oxidized counterpart indicate partial oxidation of the bismuth telluride nanoparticles.

We fabricated 300-nm-thick film assemblies of the nanocrystals from a colloidal solution by dip coating on 1-cm^2 glass substrates with prefabricated microheaters and microelectrodes for electrical and thermoelectric property measurements. Since the millimeter-scale electrodes are much larger than the micrometer-scale film thickness, we use a one-dimensional model to describe the transport properties of the film. The as-deposited Bi_2Te_3 nanocrystal films were electrically insulating as expected due to surfactant capping and surface oxidation discussed above.

Received: April 6, 2011
Revised: May 22, 2011
Published: June 01, 2011

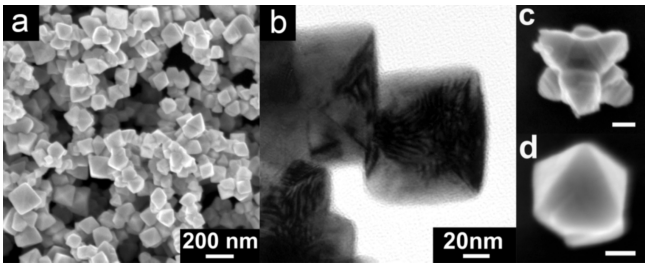

Figure 1. (a) SEM and (b) bright-field TEM images of polyhedral bismuth telluride nanocrystal polyhedra that have either (c) four or (d) eight sides. Scale bars in (c) and (d) denote 50 nm.

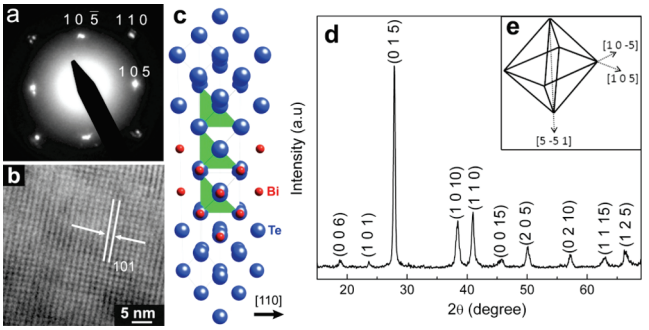

Figure 2. (a) A [5$\bar{5}$1] zone axis electron diffraction pattern and (b) a high resolution TEM image from two overlapping Bi_2Te_3 nanocrystal polyhedra. (c) Schematic sketch of the [5$\bar{5}$1] projection of the Bi_2Te_3 unit cell. (d) X-ray diffractogram from the Bi_2Te_3 nanocrystal powders. (e) A schematic sketch capturing the crystallographic morphology of the octahedrally faceted nanocrystals.

However, treating the film with hydrazine vapor followed by vacuum annealing at 300 °C renders the nanocrystal assemblies electrically conducting due to oleic acid desorption[13] and some particle coalescence. TEM micrographs from annealed films are essentially indistinguishable compared to those from as-prepared films indicating no observable microstructural changes.

The cross-plane thermal conductivity of the annealed thin film assemblies was determined to be $\kappa = 0.6 \pm 0.2$ W/mK by a scanning hot-probe technique.[14] This threefold smaller value than that of bulk Bi_2Te_3 agrees well with $\kappa = 0.54$ W/mK calculated from Maxwell's effective media theory[15] assuming an ~50% porosity indicated by SEM measurements (See Supporting Information Figure S3).

The annealed assemblies exhibit linear current−voltage characteristics symmetric about the origin, characteristic of Ohmic conduction. Film resistance decreases with increasing temperature (see Figure 4a), indicating thermally activated carrier transport. The electrical conductivity $\sigma \sim 400\ \Omega^{-1}\ m^{-1}$ is about one thousand-fold smaller than bulk Bi_2Te_3,[16] attributable to porosity. The charge carrier transport activation energy $E_a = 11.2$ meV is low compared to 100−200 meV obtained for bulk Bi_2Te_3 for the same temperature range, pointing to shallow donor levels near the conduction band. Since dopants such as sulfur or selenium[16] are not introduced, we attribute the n-type behavior to bismuth deficiency[17,18] and/or oxygen donor states due to the surface oxide. Quantitative assessment of the effects of interfaces and porosity on σ is difficult because the carrier concentration and mobility in individual nanocrystals is currently not known. However, we expect that decreased porosity and increased interfacial

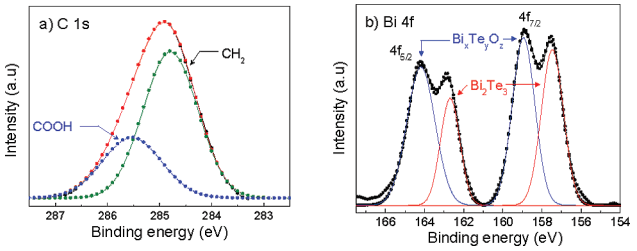

Figure 3. (a) C 1s and (b) Bi 4f core-level spectra from the Bi_2Te_3 nanocrystals. The Bi $4f_{7/2}$ and $4f_{5/2}$ bands show the presence of unoxidized as well as oxidized bismuth telluride.

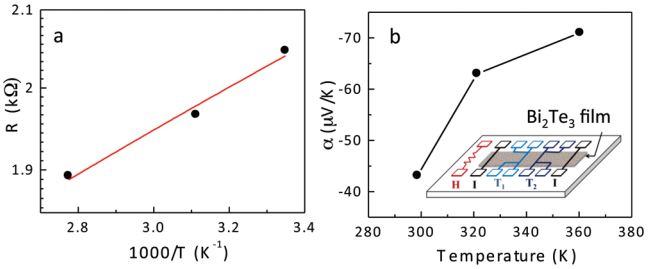

Figure 4. Temperature dependence of (a) electrical resistance R and (b) Seebeck coefficient α. Inset in (b) shows a schematic sketch of the test structure with a heat source adjacent to, and a four-probe structure patterned below, the nanoparticle film. T_1 and T_2 represent thermistors while I and H represent the current-carrying probes and heater, respectively.

contact can be realized by devising treatments to obtain high packing efficiencies possible in assemblies of faceted nanoparticles.

The Seebeck coefficient α ranges from −42 μV/K at room temperature to −73 μV/K at 360 K (Figure 4b), indicating n-type behavior. These values are about threefold lower than that of the best bulk n-type bismuth telluride selenide alloys (−230 μV/K),[16] most likely due to unoptimized carrier concentration that can be tuned by adjusting chemical composition and doping.

In summary, we have reported the solvothermal synthesis of faceted single crystal bismuth telluride nanoparticles. Thin film assemblies of these nanoparticles show threefold lower thermal conductivity than the bulk and low power-factors due to film porosity, unoptimized carrier concentration, and interparticle interfacial contact. Further refining shape selection, doping, and devising treatments to obtain the highest packing efficiencies possible in assemblies of faceted nanoparticles offer promise for enhancing thermoelectric properties.

■ ASSOCIATED CONTENT

Supporting Information. Experimental methods and synthesis procedures, size distributions of the bismuth telluride nanoparticles, a transmission electron micrograph of the nanoparticles, and a scanning electron micrograph of a thin film assembly of the nanoparticles are provided. This material is available free of charge via the Internet at http://pubs.acs.org.

■ AUTHOR INFORMATION

Corresponding Author
*E-mail: ramanath@rpi.edu.

■ ACKNOWLEDGMENT

We gratefully acknowledge funding support from the New York State Foundation for Science, Technology and Innovation (NYSTAR) and NSF Awards DMR 0519081 and CBET-0348613.

■ REFERENCES

(1) Dresselhaus, M. S.; Chen, G.; Tang, M. Y.; Yang, R. G.; Lee, H.; Wang, D. Z.; Ren, Z. F.; Fleurial, J. P.; Gogna, P. *Adv. Mater.* **2007**, *19*, 1043–1053.

(2) Chen, G.; Dresselhaus, M. S.; Dresselhaus, G.; Fleurial, J. P.; Caillat, T. *Int. Mater. Rev.* **2003**, *48*, 45–66.

(3) Hicks, L. D.; Dresselhaus, M. S. *Phys. Rev. B* **1993**, *47*, 12727–12731.

(4) Harman, T. C.; Reeder, R. E.; Walsh, M. P.; LaForge, B. E.; Hoyt, C. D.; Turner, G. W. *Appl. Phys. Lett.* **2006**, *88*, 243504−1–243504−3.

(5) Venkatasubramanian, R.; Siivola, E.; Colpitts, T.; O'Quinn, B. *Nature* **2001**, *413*, 597–602.

(6) Wang, R. Y.; Feser, J. P.; Lee, J. S.; Talapin, D. V.; Segalman, R.; Majumdar, A. *Nano Lett.* **2008**, *8*, 2283–2288.

(7) Poudel, B.; Hao, Q.; Ma, Y.; Lan, Y. C.; Minnich, A.; Yu, B.; Yan, X.; Wang, D. Z.; Muto, A.; Vashaee, D.; Chen, X. Y.; Liu, J. M.; Dresselhaus, M. S.; Chen, G.; Ren, Z. *Science* **2008**, *320*, 634–638.

(8) Haskins, J. B.; Kinaci, A.; Cagin, T. *Nanotechnology* **2011**, *22*, 155701-1–155701-7.

(9) Skrabalak, S. E.; Xia, Y. A. *ACS Nano* **2009**, *3*, 10–15.

(10) Song, Q.; Ding, Y.; Wang, Z. L.; Zhang, Z. J. *J. Phys. Chem. B* **2006**, *110*, 25547–25550.

(11) Huheey, J. E.; Keiter, E. A.; Keiter, R. L. *Inorganic Chemistry: Principles of Structure and Reactivity*, 4th ed.; Prentice Hall: 1997.

(12) JCPDS card number 08-0027

(13) Talapin, D. V.; Murray, C. B. *Science* **2005**, *310*, 86–89.

(14) Zhang, Y. L.; Hapenciuc, C. L.; Castillo, E. E.; Borca-Tasciuc, T.; Mehta, R. J.; Karthik, C.; Ramanath, G. *Appl. Phys. Lett.* **2010**, *96*, 062107−1–062107−3.

(15) Hasselman, D. P. H.; Johnson, L. F. *J. Compos. Mater.* **1987**, *21*, 508–515.

(16) Rowe, D. M. *Thermoelectrics Handbook: Macro to Nano*; CRC Press: Boca Raon, FL, 2005.

(17) Li, S. H.; Toprak, M. S.; Soliman, H. M. A.; Zhou, J.; Muhammed, M.; Platzek, D.; Muller, E. *Chem. Mater.* **2006**, *18*, 3627–3633.

(18) Zhao, L. D.; Zhang, B. P.; Li, J. F.; Zhang, H. L.; Liu, W. S. *Solid State Sci.* **2008**, *10*, 651–658.